doi: 10.4149/gpb_2022007

Junctophilin-2 allosterically interacts with ryanodine receptor type 2 to regulate calcium release units in mouse cardiomyocytes

Tianxia Luo[1,2], Ningning Yan[2], Mengru Xu[2], Fengjuan Dong[2], Qian Liang[2], Ying Xing[2] and Hongkun Fan[2]

[1] *Department of Physiology, School of Medicine, Henan University of Chinese Medicine, Zhengzhou, China*
[2] *Department of Physiology and Neurobiology, School of Basic Medical Sciences, Zhengzhou University, Zhengzhou, China*

Abstract. The interaction between junctophilin-2 (JPH2) and ryanodine receptor type 2 (RyR2) regulated Ca^{2+} signaling in mouse cardiomyocytes. However, their exact interaction remains unclear. This study elucidates the interaction between JPH2 with RyR2 using co-immunoprecipitation of cardiac sarcoplasmic reticulum vesicles. Additionally, a glutathione S-transferase (GST) pull-down analysis was performed to investigate the physical interaction between RyR2 and JPH2 fragments. JPH2 interacted with RyR2 and the C terminus of the JPH2 protein can pull-down RyR2 receptors. Confocal immunofluorescence imaging indicated that the majority of JPH2 and RyR2 proteins were colocalized near Z-lines in isolated mouse cardiomyocytes. Knockdown of JPH2 reduced the amplitude of Ca^{2+} transients and disrupted its interaction with RyR2. Therefore, the C-terminus domain of JPH2 is required for interactions with RyR2 in mouse cardiomyocytes, which provides a molecular mechanism for seeking Ca^{2+}-related disease prevention strategies.

Key words: Junctophilin-2 — Ryanodine receptor type 2 — Cardiomyocytes — Ca^{2+} release

Introduction

Ryanodine receptors (RyRs) are mediate Ca^{2+} release channels from stores of intracellular Ca^{2+}, such as endoplasmic reticulum (ER) or sarcoplasmic reticulum (SR) (Nabauer et al. 1989; Dulhunty 1992; Rios et al. 1992; Giannini et al. 1995). RyR1 is expressed in skeletal muscle, whereas RyR2 is predominantly expressed in cardiac muscle, and RyR3 is ubiquitously expressed in parotid acinar cells, the central nervous system, and skeletal muscle (Dulhunty 1992; Rios et al. 1992; Giannini et al. 1995). In striated muscle, membrane depolarization activates the voltage-gated Ca^{2+} channels (VGCC) in the plasma membrane (PM) inducing a great Ca^{2+} release from the SR *via* RyR1 and RyR2, and subsequently inducing a muscle contraction (Dulhunty 1992; Rios et al. 1992). The Ca^{2+}-induced Ca^{2+} release in cardiomyocytes occurs mainly in the diad, a system of tubules distributed around the myofibrils, and is associated with the formation of T-tubules, invaginations of the PM, which are closely juxtaposed with a single terminal cistern of the ER/SR (Dulhunty 1992; Rios et al. 1992; Franzini-Armstrong 2009). Junctophilins (JPHs) interact with VGCC and RyRs to regulate Ca^{2+} homoeostasis and help induce excitation-contraction coupling in muscles (Lee et al. 2006; Woo et al. 2008, 2009; Golini et al. 2011).

JPHs belong to a family of junctional membrane complexes. They are located between the PM and ER membranes to facilitate contact between the two membranes in all excitable cells (Takeshima et al. 2000). Skeletal muscles express both JHP1 and JPH2; cardiac muscles only express JPH2; while JPH3 and JPH4 are mainly expressed across various components of the central nervous system (Takeshima et al. 2000; Garbino et al. 2009). All JPHs contain eight membrane occupation and recognition nexus (MORN) domains, which are able to interact with the

Correspondence to: Hongkun Fan, Department of Physiology and Neurobiology, School of Basic Medical Sciences, Zhengzhou University, No.100 Kexuedadao Road, Zhengzhou, 450000, Henan, China
E-mail: fanhk@zzu.edu.cn

PM, and are followed by an α-helical region, a divergent region, and include C-terminal domain anchoring proteins that are located in the ER/SR (Takeshima et al. 2000, 2015). In mice, JPH2 knockout is lethal in the embryonic phase, which is attributed to heart failure (HF) that is caused by the decoupling of the excitation-contraction in the muscles. Therefore, JPH2 is essential for the functional crosstalk between VGCC and RyR2 for proper functioning of the embryonic heart (Takeshima et al. 2000). As JPH2 was downregulated in cases of cardiomyopathy and HF, it was found that subsequent induction of the overexpression of JPH2 corrected cardiac function in mice with early stage HF. The overexpression inhibited SR Ca^{2+} leaks induced by RyR2 (Landstrom et al. 2011; Reynolds et al. 2016). Quantitative single-molecule localization microscopy also indicated that colocalization between RyR2 and JPH2 in JPH2 knockdown cardiomyocytes was reduced. In contrast, in cases of induced overexpression of JPH2 in cardiomyocytes, RyR2 colocalized with JPH2 at significantly increased levels (Munro et al. 2016). However, the binding domain between JPH2 and RyR2 channels has not been fully elucidated.

In the present study, we sought to further examine the molecular regulation of RyR2 channels by the JPH2 in mouse cardiomyocytes and determine whether interaction sites were localized to the C-terminus of JPH2 proteins.

Methods

Animals

We used 3-month-old mature C57BL/6 mice of both sexes obtained from Beijing Weitong Lihua Experimental Animal Technology, Limited, China (No. SCXK Jing 2012-0001). Ethics for animal care followed guidelines from the Committee on the Ethics of Animal Experiments of the University of Zhengzhou, China (No. SYXK-2010-0001). Procedures for experimental use of animals followed guidelines from the National Institutes of Health and Institution. All mice were group housed on 12 h light/dark cycles with food and water available *ad libitum*.

Plasmids construction

Three glutathione S-transferase (GST)-JPH2 fragment plasmids GST-JPH2-N1 (aa1–253), GST-JPH2-N2 (aa216–350), and GST-JPH2-C (aa340–696) were subcloned into the pGEX-4T-1 vector and the accuracy of the plasmids was verified as previously described (Fan et al. 2018).

Cardiac SR membrane vesicles isolation

Cardiac SR membrane vesicles were isolated by differential centrifugation, as previously described (Schilling and Lindenmayer 1984; Lee et al. 2004). All mice were anesthetized with sodium pentobarbital (50 mg/kg, intraperitoneal injection) and euthanized by thoracotomy. Whole hearts were removed by careful dissection and stored at −80°C. The hearts were minced and homogenized in a cold lysis buffer containing 0.25 M sucrose, 10 M Tris-HCl (pH 7.0), and 1 mM EDTA. Individual homogenates were centrifuged at 5,000 × *g* for 10 min. The supernatant was removed, and samples were centrifuged at 40,000 × *g* for 45 min. The resultant pellet that was representative of the SR vesicles was suspended in 0.6 M KCl solution and centrifuged at 40,000 × *g* for 45 min. The pellet was suspended in cold lysis buffer and stored at −80°C until further use.

Co-immunoprecipitation

We examined the interaction between JPH2 and RyR2 in SR vesicles using co-immunoprecipitation assays. The solubilized proteins from SR vesicle lysis of the infected adult mouse myocardium were incubated with anti-JPH2 (cat. no. PRS4919; Sigma-Aldrich, St. Louis, MS, USA) or anti-RyR2 antibodies (cat. no. MA3-916; Thermo Fisher Scientific, Waltham, MA, USA) at 4°C overnight, followed by incubation with protein A/G sepharose (Santa Cruz Biotechnology, Dallas, TX, USA) for 6 h at 4°C. Next, the beads were washed for 10 min with washing buffer, collected after each wash, and resuspended in the SR vesicle sample buffer by boiling for 5 min. Extracted precipitated proteins were used for SDS-PAGE and Western blot analysis.

GST pull-down assays

Construction of the GST-JPH2 fragment plasmids and implementation of GST pull-down assays were performed in our previous study (Fan et al. 2018). Briefly, plasmids were transformed into *E. coli* BL-21 (DE3) and were introduced into samples using 0.1 mM isopropyl-β-D-thiogalactoside at 20°C with 40 rpm overnight. The resultant immobilized GST, GST-JPH2-N1, GST-JPH2-N2, and GST-JPH2-C were incubated with the protein samples prepared from SR vesicles at 4°C overnight. The pulldown complexes were eluted using the elution buffer as part of the Pierce™ GST Protein Interaction Pull-Down Kit (Thermo Fisher Scientific, Waltham, MA, USA). The eluted products were boiled for 5 min at 95°C and analyzed by Western blot.

Single cardiomyocyte isolation

Single cardiomyocyte samples were prepared as described in a previous study (Fan et al. 2018). After the anesthesia and subsequent euthanized, whole hearts from adult mice were rapidly dissected and washed with ice-cold Ca^{2+}-free

modified Tyrode's solution (140 mM NaCl, 5.4 mM KCl, 1 mM $MgCl_2$, 10 mM HEPES, and 10 mM glucose at pH 7.4). Each heart sample was cannulated and mounted onto a Langendorff perfusion system, perfused with a fresh enzyme solution (collagenase type II and protease) for 35 min, and then subjected to a high K^+ solution (120 mM potassium glutamate, 20 mM KCl, 1 mM $MgCl_2$, 0.3 mM EGTA, 10 mM glucose, and 10 mM HEPES; adjusted to pH 7.4 with KOH) for 5 min. Single atrial and ventricular cells were isolated and kept within the high K^+ solution before we performed immunocytochemistry and measurements of the Ca^{2+} transients.

Immunocytochemistry

Single atrial and ventricular cells were fixed in 4% paraformaldehyde for 30 min, treated with 0.4% Triton X-100 for 15 min, washed, and incubated with anti-RyR2 antibody or anti-JPH2 antibody at 4°C overnight. Cells were incubated with FITC-conjugated goat anti-mouse antibody (Jackson ImmunoResearch, West Grove, PA, USA) or incubated with TRITC-conjugated goat anti-rabbit antibody (Jackson ImmunoResearch) for 1 h. An Olympus FV1000 confocal laser scanning microscope (Shinjuku City, Tokyo, Japan) was used to visualize fluorescence signals.

JPH2 knockdown by RNA interference

Oligonucleotides encoding shRNA (GTATGGTGATCTTGCTGAA), and the negative control shRNA (TTCTCCGAACGTGTCACGT) used in our study, were previously successfully constructed. We applied a total dose of 1×10^9 PFU adenovirus with control siRNA and JPH2 siRNA into the mice, as previously described Fan et al. (2018). At the end of the experiment, all mice were anesthetized and the hearts were removed.

To determine quantitative levels of JPH2 and RyR2 mRNA expression, total RNA was isolated from the infected myocardium using Trizol (Thermo Fisher Scientific) and was analyzed using real-time PCR as previously described (Mu et al. 2014). The PCR primers used to detect the expression levels of JPH2, RyR2, and GAPDH are listed in Table 1. Each primer set was designed and synthesized by Shanghai GeneChem Biotechnology (Shanghai, China). The relative gene expression levels of JPH2 and RyR2 were normalized to those of GAPDH mRNA expression levels were calculated using the $2^{-\Delta\Delta Ct}$ method.

To determine the expression levels of JPH2 and RyR2 proteins, infected mouse myocardium samples were lysed in RIPA buffer. Total protein concentrations were determined using a BCA kit (Thermo Fisher Scientific, Waltham, MA, USA). Precipitated proteins were analyzed using Western blotting.

We applied co-immunoprecipitation in adult mouse myocardium infected with a vector and small interfering RNA (Ad-NC-siRNA and Ad-JPH2-siRNA). The expression of RyR2 channels in the immunoprecipitation complex was detected by Western blotting.

Ca^{2+} transient measurements

The mice were transfected with the adenovirus vector through specific siJPH2 tail vein injection (Ad-siJPH2). Infected adult cardiomyocytes were incubated with 2 μmol/l fura-2 for 30 min at 37°C, and then washed twice with Tyrode's solution containing 1.8 mmol/l $CaCl_2$. We stimulated cells at 1.0 Hz using field stimulation to evoke Ca^{2+} transients. Intracellular Ca^{2+} levels were determined by calculating the 340/380 nm ratio of fura-2 fluorescence excited at 510 nm using an IonOptix photometry system (PMT-300, USA). The SR-based calcium content in the cells was determined using 10 mM caffeine. Data were collected and analyzed using SignalAverager Software IonWizard 6.6 (IonOptix), with all parameters set to manufacture defaults.

Statistical analysis

Data are expressed as the mean ± standard error of the mean (SEM). Differences between the treatment groups were evaluated using one-way ANOVA followed by paired or unpaired Student's *t*-tests, as appropriate. Differences were considered significant when the p values were < 0.05.

Results

JPH2 associates with RyR2 receptors in the cardiac membrane SR vesicles

Solubilized proteins from SR vesicles were immunoprecipitated using the anti-RyR2 antibody and subsequently immunoblotted using the anti-JPH2 antibody, and RyR2 was observed to selectively bind to endogenous JPH2 in the SR vesicles (Fig. 1A, left). Similarly, in the reverse co-

Table 1. Primers used to amplify JPH2, RyR2 and GAPDH

Gene	Primer sequences	
JPH2	Forward	5'-CTGGCTATCCATTTGTTCACCT-3'
	Reverse	5'-GTTTTAGGTCCGAAGTCCCAT-3'
RyR2	Forward	5'-GAATTCATCATGGATACTCTACC-3'
	Reverse	5'-GTCATGCACATTATCTTCTGCAT-3'
GAPDH	Forward	5'-GGTTGTCTCCTGCGACTTCA-3'
	Reverse	5'-TGGTCCAGGGTTTCTTACTCC-3'

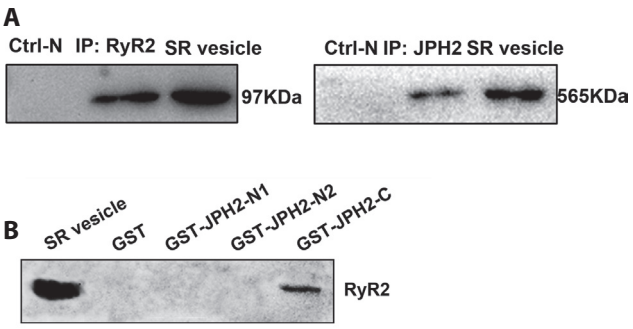

Figure 1. Interaction between JPH2 and RyR2 in isolated cardiac sarcoplasmic reticulum (SR) membrane vesicles. **A.** SR vesicles were solubilized and subjected to immunoprecipitation (IP) with antibodies to RyR2 or JPH2. The soluble proteins extracted from cardiac SR vesicles were used as positive control, and Ctrl-N was negative control using a non-immobilized gel. **B.** Purified GST or GST-JPH2 fragment fusion proteins containing GST-JPH2-N1, GST-JPH2-N2 and GST-JPH2-C were immobilized and detected with anti-RyR2 antibody using GST pull down assay.

immunoprecipitation experiments using the anti-RyR2 antibody (Fig. 1A, right), the JPH2 protein specifically bound to RyR2, whereas no specific immunoreaction was observed using an unrelated antibody (Fig. 1A, left and right panels). These results imply a specific interaction between JPH2 and RyR2 in the native cardiac tissue.

We further observed JPH2 selectively bound to RyR2. As shown in Figure 1B, JPH2-C (aa340–696 containing the C-terminal region of JPH2) selectively bound to RyR2. However, GST alone, GST-JPH2-N1, and GST-JPH2-N2 did not interact with RyR2. Our data indicated that the JPH2-C domain contains the majority of the binding sites for the RyR2 receptor *in vitro*, suggesting that this is a preliminary structural requirement for JPH2 to link to RyR2.

Colocalization of JPH2 and RyR2 in adult mouse cardiomyocytes

To determine whether JPH2 and RyR2 proteins were colocalized in cardiomyocytes, we performed immunofluorescence staining of isolated mouse cardiomyocytes. Figures 2A and 2B indicate that JPH2 and RyR2 maintained the same patterns of striation in single isolated cardiac cells, even in areas where Z-lines were present in the ventricular myocytes (Fig. 2B), or areas with Z-tubules in the atrial myocytes (Fig. 2A). Results from controls, in which staining with the secondary antibodies were used, indicated that co-localization of JPH2 and RyR2 in cardiomyocytes was a valid result (Fig. 2C).

Knockdown of JPH2 disrupts its interaction with RyR2

After transfection with the adenovirus vector through specific siJPH2 tail vein injection (Ad-siJPH2), the levels of JPH2 mRNA (Fig. 3A) and proteins (Fig. 3C,D) in the adult mouse myocardium were significantly suppressed compared with the control groups (Ad-NC). However, the knockdown of JPH2 did not alter the mRNA (Fig. 3B) or protein (Fig. 3E,F) levels of RyR2.

To examine whether knockdown of JPH2 disrupted the binding between the JPH2 and RyR2 proteins, we applied co-immunoprecipitation in infected adult mouse myocardium, and observed the expression of RyR2 channels. Figure 4A and 4B shows that compared with the negative control myocardium, the expression of the RyR2 channels pulled down by JPH2 was significantly decreased in the mouse myocardium infected with Ad-siJPH2. These results suggest that JPH2 knockdown may affect its binding to RyR2 channels.

Knockdown of JPH2 depresses intracellular Ca^{2+} transients

To test whether JPH2 modulated RyR2 receptor function, we used the approach of RNA-based interference and recorded

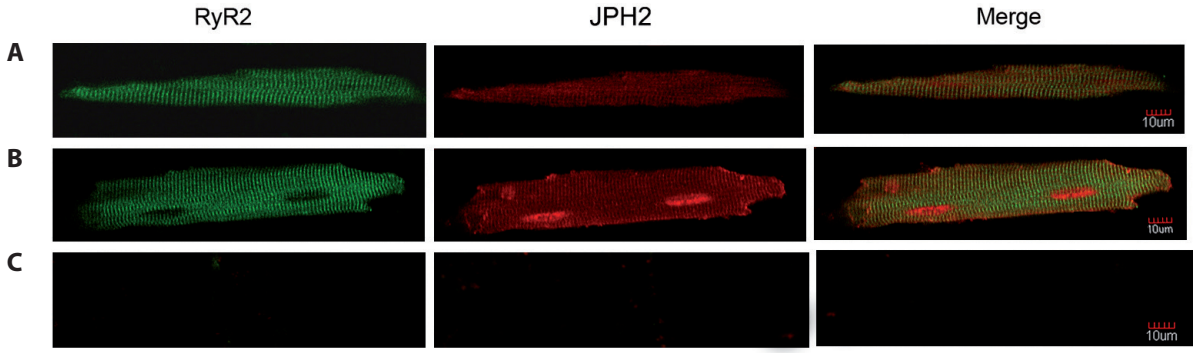

Figure 2. Co-localization of JPH2 and RyR2 in mouse cardiomyocytes. Immunofluorescent staining showed dual immunolabelling of JPH2 (red) with RyR2 (green) in single isolated atrial (**A**) and ventricular (**B**) myocytes. **C.** Negative control experiments were performed with the secondary antibodies in atria myocytes. Scale bars, 10 μm. For color figure, see online manuscript.

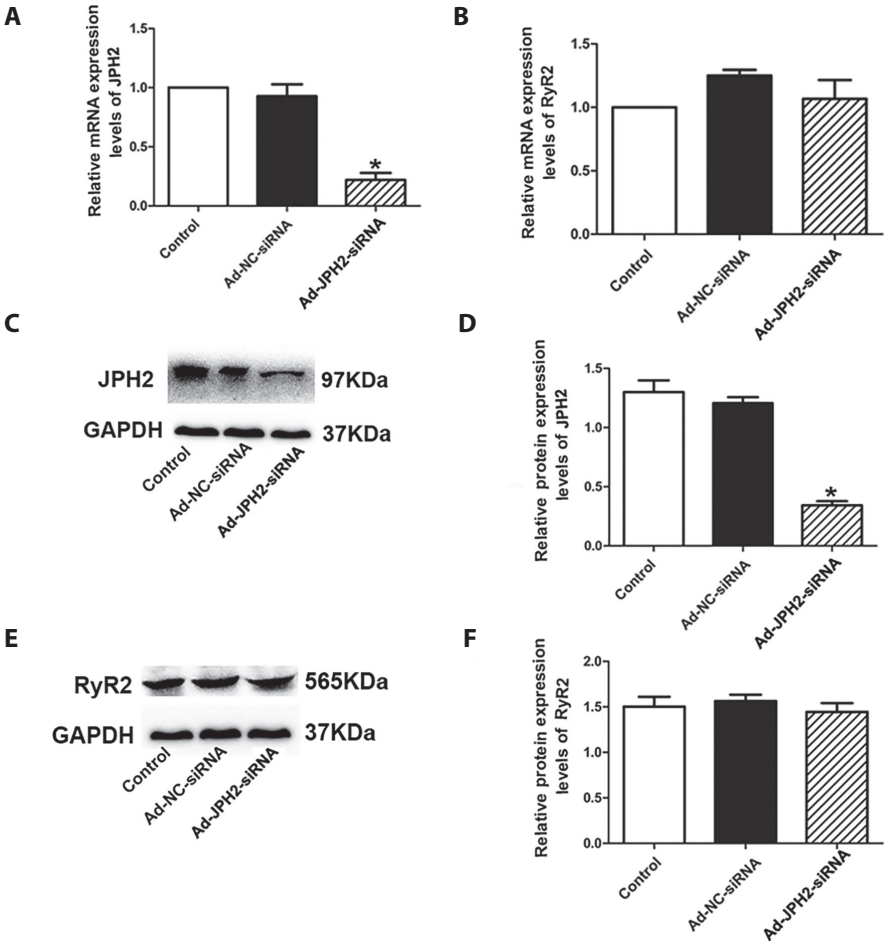

Figure 3. Knockdown of JPH2 did not change the expression of RyR2. **A.** The bar graphs show significant decrease in JPH2 mRNA of myocardium infected by adenovirus vector with specific JPH2 siRNA (Ad-JPH2-siRNA), compared with control groups. **B.** The bar graphs show RyR2 mRNA did not change in myocardium with different treatments. **C.** Western blotting analysis of JPH2 expression in different treatments. **D.** The bar graphs show significant downregulation of JPH2 protein expression after infection of JPH2 siRNA. **E.** A representative Western blotting analysis showing RyR2 expression in myocardium with different treatments. **F.** The bar graphs show no significant change of RyR2 mRNA expression after infection of JPH2 siRNA. Error bars represent ± SEM; * $p < 0.05$ *vs.* control group; Student's *t*-test.

levels of intracellular Ca^{2+} transients. Typical recordings of intracellular Ca^{2+} transients in infected cardiomyocytes are revealed in Figure 5A. The amplitude of Ca^{2+} transients was significantly decreased in the treatment of cells transfected with JPH2 siRNA (0.33 ± 0.02, $n = 36$) compared with the control cells (0.52 ± 0.16, $n = 36$, $p < 0.05$) (Fig. 5C). The resting calcium levels were unchanged in the cardiac myocytes infected with Ad-siJPH2 compared with the control cells (1.15 ± 0.26 *vs.* 1.19 ± 0.24, $p = 0.30$, $n = 30$) (Fig. 5B). We further investigated whether JPH2 knockdown interfered with the function of the RyR2 receptor. Similar results demonstrated that the amplitude of Ca^{2+} transients was significantly decreased in the Ad-siJPH2 treatment group compared with the control group, where we used 10 mmol/l caffeine in the cell suspension (0.51 ± 0.02 *vs.* 0.87 ± 0.03, $n = 32$, $p < 0.05$) (Fig. 5D).

Discussion

JPH2 is the cardiac isoform of the junctophilin family and acts as a molecular bridge for signal transduction by anchoring the PM and ER/SR membrane systems (Takeshima et al. 2000). In the present study, mouse cardiac SR membrane vesicles were isolated by differential separation, and specific

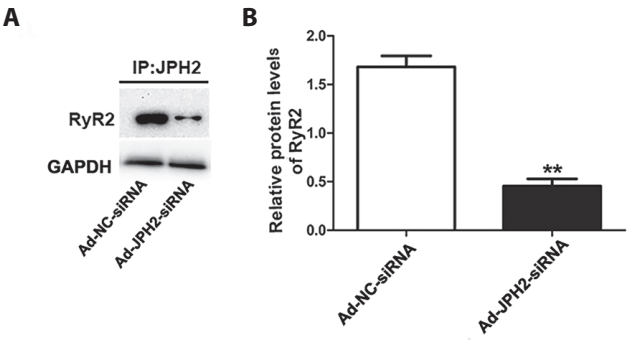

Figure 4. JPH2 knockdown decrease its binding with RyR2 channel. **A.** Protein immunoprecipitated (IP) with JPH2 antibody from adult mouse myocardium infected with Ad-NC-siRNA and Ad-JPH2-siRNA was detected by Western blot using RyR2 antibody. **B.** Relative protein level of RyR2 channel. ** $p < 0.01$.

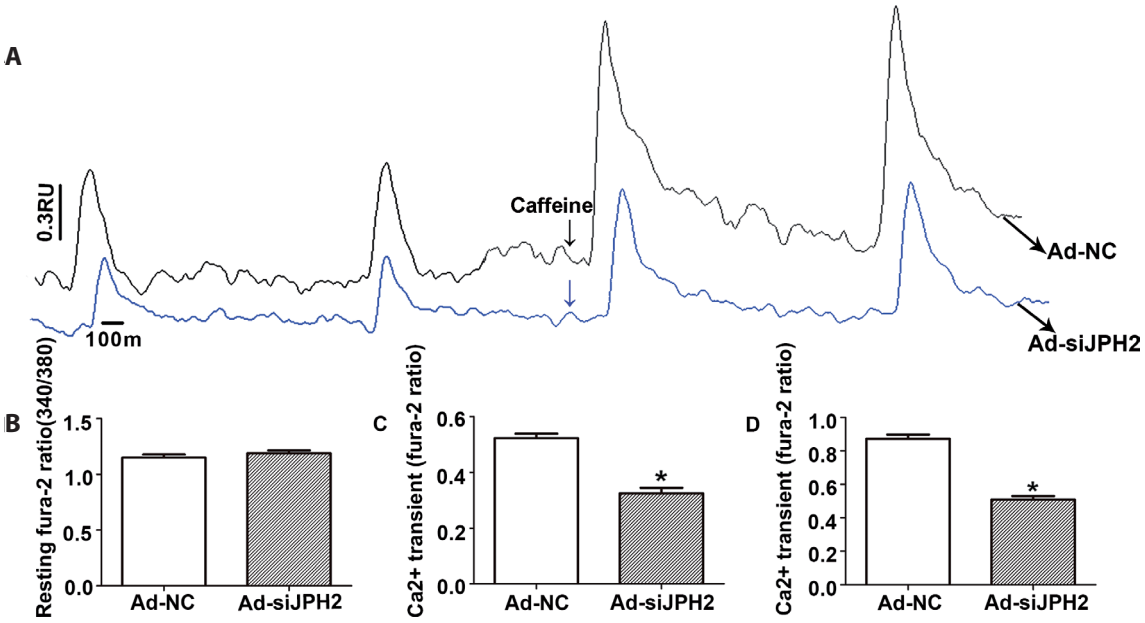

Figure 5. Knockdown of JPH2 depresses Ca^{2+} transient in mouse cardiomyocytes. **A.** The curves of the Ca^{2+} transient of fura-2 loaded adult mouse cardiac myocytes. The black curve represents the negative control (Ad-NC), the blue curve is cells transfected by adenovirus vector with specific JPH2 siRNA (Ad-siJPH2). **B.** The bar graphs of resting fura-2 ratio in Ad-siJPH2 infected mouse cardiac myocytes ($n = 30$ *per* group). **C.** The bar graphs of the amplitude of the $[Ca^{2+}]i$ transient in Ad-siJPH2 infected mouse cardiac myocytes ($n = 36$ *per* group). **D.** The bar graphs of Ca^{2+} transients elicited by application of 10 mM caffeine ($n = 32$ *per* group). Error bars represent ± SEM; * $p < 0.05$ *vs.* control group; Student's *t*-test.

anti-JPH2 and anti-RyR2 antibodies recognized JPH2 and RyR2 in the SR vesicles.

JPH2 has previously been suggested to interact with RyR2 and Cav1.2, to regulate their gating channel functions (van Oort et al. 2011; Li et al. 2013). Previous observations suggested that both JPH2 and RyR2 labeling puncta strongly overlapped, and that the amount of JPH2 associated with RyR2 clusters was greatly reduced after JPH2 manual knockdown (Jayasinghe et al. 2012; Munro et al. 2016). In the present study, the results of co-immunoprecipitation assays suggested that RyR2 interacted with JPH2 proteins in SR vesicles, and confocal immunofluorescence imaging analysis suggested that the majority of both JPH2 and RyR2 proteins were colocalized near Z-lines in adult mouse cardiomyocytes. Thus, we provided further evidence that JPH2, a member of the JMC family of proteins found in cardiomyocytes, interacts with RyR2 receptors.

Previous research has predicted that JPHs have a short C-terminal domain that is important for anchoring proteins into the ER/SR, as well as repeated N-terminal MORN domains that are able to interact with the PM, thereby causing a junctional association of these two membrane systems (Takeshima et al. 2000). Results from a related study indicated that the N-terminal domain of JPH2 is responsible for the physical and functional interaction with the small-conductance Ca^{2+}-activated K^+ channel subtype 2 (SK2) in the PM (Fan et al. 2018). We found that the region of JPH2 (aa340-696) interacted with RyR2 in mouse cardiomyocytes. Recent reports have suggested that the N-terminal region of JPH2 (aa1–565) interacted with RyR2 and Cav1.2, but does not interact with the C terminus region of JPH2 (aa566–end), indicating that it was not sufficient to restore Ca^{2+} transients in JPH2 knockdown cardiomyocytes (Guo et al. 2015). Based on the different cleavage products found in the study, we concluded that the overlapping region 340–565 may contain the determinants for the binding between JPH2 and RyR2. In another study, Beavers et al. (2013) found that the E169K mutation in JPH2 specifically disrupts its binding domain with RyR2 due to perturbed Ca^{2+} handling, indicating that residue E169 within a crucial domain of JPH2 modulates the RyR2 channel. The E169 residue in JPH2 is located in a flexible "joining domain" between two MORN domains, which attaches JPH2 to the sarcolemma (Takeshima et al. 2000; Garbino et al. 2009).

Recent studies have also demonstrated that the cardiac-specific knockdown of JPH2 triggers an SR Ca^{2+} leak by directly increasing the probability of open RyR2 receptors in cardiomyocytes (van Oort et al. 2011; Beavers et

al. 2013; Munro et al. 2016). Moreover, downregulation of JPH2 has been observed in patients with hypertrophic cardiomyopathy. In some rodent-based model analyses of hypertrophic cardiomyopathy, overexpression of JPH2, which could correct cardiac function with early stage HF, is used to inhibit SR Ca^{2+} leaks induced by RyR2 (Landstrom et al. 2011; Reynolds et al. 2016). Thus, these results suggest that JPH2 modulates intracellular Ca^{2+} handling through the regulation of RyR2. In the present study, we further confirmed that siRNA-based knockdown of JPH2 resulted in reduced amplitudes of Ca^{2+} transients in cardiomyocytes, but the respective levels of RyR2 mRNA and proteins showed no significant change in our reports. This result is consistent with previous findings from similar analyses by the authors of this study and others (van Oort et al. 2011; Beavers et al. 2013; Munro et al. 2016; Fan et al. 2018). It was likely a result of decreasing levels of SR Ca^{2+} stores, which resulted in a SR Ca^{2+} leak by directly increasing the probability that RyR2 receptors would be open.

To summarize, our data confirm that JPH2 plays a critical role in regulating intracellular calcium levels by binding to, and modulating, RyR2 through its C-terminal domain. Nevertheless, further research is warranted to unequivocally evaluate the specific mechanisms by which JPH2 proteins influence RyR2 channel function *in vivo*. This would be useful to determine the direct link between aberrant ion channel function and cardiac arrhythmias.

In conclusion, we provide more insights into the possible functional regulation of RyR2 channels by the JPH2 protein and prove that the interaction sites were localized to the C-terminus of JPH2 proteins. This consequently plays an important role in maintaining intracellular calcium homeostasis and excitation-contraction coupling, which provides a molecular mechanism for seeking Ca^{2+}-related disease prevention strategies.

Acknowledgements. This study was funded by National Natural Science Foundation of China (No. 81570311 and 81270248) and Doctoral Scientific Research of Henan University of Chinese Medicine (00104311-2021-1-144).

Conflict of interest. The authors declare that they have no conflicts of interest.

References

Beavers DL, Wang W, Ather S, Voigt N, Garbino A, Dixit SS, Landstrom AP, Li N, Wang Q, Olivotto I, et al. (2013): Mutation E169K in junctophilin-2 causes atrial fibrillation due to impaired RyR2 stabilization. J. Am. Coll. Cardiol. **62,** 2010-2019 https://doi.org/10.1016/j.jacc.2013.06.052

Dulhunty AF (1992): The voltage-activation of contraction in skeletal muscle. Prog. Biophys. Mol. Biol. **57,** 181-223 https://doi.org/10.1016/0079-6107(92)90024-Z

Fan HK, Luo TX, Zhao WD, Mu YH, Yang Y, Guo WJ, Tu HY, Zhang Q (2018): Functional interaction of Junctophilin 2 with small-conductance Ca(2+)-activated potassium channel subtype 2(SK2) in mouse cardiac myocytes. Acta Physiol. (Oxf.) **222,** e12986 https://doi.org/10.1111/apha.12986

Franzini-Armstrong C (2009): Architecture and regulation of the Ca2+ delivery system in muscle cells. Appl. Physiol. Nutr. Metab. **34,** 323-327 https://doi.org/10.1139/H09-017

Garbino A, van Oort RJ, Dixit SS, Landstrom AP, Ackerman MJ, Wehrens XH (2009): Molecular evolution of the junctophilin gene family. Physiol. Genomics **37,** 175-186 https://doi.org/10.1152/physiolgenomics.00017.2009

Giannini G, Conti A, Mammarella S, Scrobogna M, Sorrentino V (1995): The ryanodine receptor/calcium channel genes are widely and differentially expressed in murine brain and peripheral tissues. J. Cell. Biol. **128,** 893-904 https://doi.org/10.1083/jcb.128.5.893

Golini L, Chouabe C, Berthier C, Cusimano V, Fornaro M, Bonvallet R, Formoso L, Giacomello E, Jacquemond V, Sorrentino V (2011): Junctophilin 1 and 2 proteins interact with the L-type Ca2+ channel dihydropyridine receptors (DHPRs) in skeletal muscle. J. Biol. Chem. **286,** 43717-43725 https://doi.org/10.1074/jbc.M111.292755

Guo A, Hall D, Zhang C, Peng T, Miller JD, Kutschke W, Grueter CE, Johnson FL, Lin RZ, Song LS (2015): Molecular determinants of calpain-dependent cleavage of junctophilin-2 protein in cardiomyocytes. J. Biol. Chem. **290,** 17946-17955 https://doi.org/10.1074/jbc.M115.652396

Jayasinghe ID, Baddeley D, Kong CH, Wehrens XH, Cannell MB, Soeller C (2012): Nanoscale organization of junctophilin-2 and ryanodine receptors within peripheral couplings of rat ventricular cardiomyocytes. Biophys. J. **102,** L19-21 https://doi.org/10.1016/j.bpj.2012.01.034

Landstrom AP, Kellen CA, Dixit SS, van Oort RJ, Garbino A, Weisleder N, Ma J, Wehrens XH, Ackerman MJ (2011): Junctophilin-2 expression silencing causes cardiocyte hypertrophy and abnormal intracellular calcium-handling. Circ. Heart Fail. **4,** 214-223 https://doi.org/10.1161/CIRCHEARTFAILURE.110.958694

Lee EH, Rho SH, Kwon SJ, Eom SH, Allen PD, Kim DH (2004): N-terminal region of FKBP12 is essential for binding to the skeletal ryanodine receptor. J. Biol. Chem. **279,** 26481-26488 https://doi.org/10.1074/jbc.M309574200

Lee EH, Cherednichenko G, Pessah IN, Allen PD (2006): Functional coupling between TRPC3 and RyR1 regulates the expressions of key triadic proteins. J. Biol. Chem. **281,** 10042-10048 https://doi.org/10.1074/jbc.M600981200

Li RC, Tao J, Guo YB, Wu HD, Liu RF, Bai Y, Lv ZZ, Luo GZ, Li LL, Wang M, et al. (2013): In vivo suppression of microRNA-24 prevents the transition toward decompensated hypertrophy in aortic-constricted mice. Circ. Res. **112,** 601-605 https://doi.org/10.1161/CIRCRESAHA.112.300806

Mu YH, Zhao WC, Duan P, Chen Y, Zhao WD, Wang Q, Tu HY, Zhang Q (2014): RyR2 modulates a Ca2+-activated K+ current in mouse cardiac myocytes. PLoS One **9,** e94905

https://doi.org/10.1371/journal.pone.0094905
Munro ML, Jayasinghe ID, Wang Q, Quick A, Wang W, Baddeley D, Wehrens XH, Soeller C (2016): Junctophilin-2 in the nanoscale organisation and functional signalling of ryanodine receptor clusters in cardiomyocytes. J. Cell. Sci. **129,** 4388-4398
https://doi.org/10.1242/jcs.196873
Nabauer M, Callewaert G, Cleemann L, Morad M (1989): Regulation of calcium release is gated by calcium current, not gating charge, in cardiac myocytes. Science (New York) **244,** 800-803
https://doi.org/10.1126/science.2543067
Reynolds JO, Quick AP, Wang Q, Beavers DL, Philippen LE, Showell J, Barreto-Torres G, Thuerauf DJ, Doroudgar S, Glembotski CC, Wehrens XH (2016): Junctophilin-2 gene therapy rescues heart failure by normalizing RyR2-mediated Ca(2+) release. Int. J. Cardiol. **225,** 371-380
https://doi.org/10.1016/j.ijcard.2016.10.021
Rios E, Pizarro G, Stefani E (1992): Charge movement and the nature of signal transduction in skeletal muscle excitation-contraction coupling. Annu. Rev. Physiol. **54,** 109-133
https://doi.org/10.1146/annurev.ph.54.030192.000545
Schilling WP, Lindenmayer GE (1984):Voltage-sensitive calcium flux promoted by vesicles in an isolated cardiac sarcolemma preparation. J. Membr. Biol. **79,** 163-173
https://doi.org/10.1007/BF01872120
Takeshima H, Komazaki S, Nishi M, Iino M, Kangawa K (2000): Junctophilins: a novel family of junctional membrane complex proteins. Mol. Cell **6,** 11-22
https://doi.org/10.1016/S1097-2765(05)00005-5
Takeshima H, Hoshijima M, Song L (2015): Ca(2)(+) microdomains organized by junctophilins. Cell. Calcium **58,** 349-356
https://doi.org/10.1016/j.ceca.2015.01.007
van Oort RJ, Garbino A, Wang W, Dixit SS, Landstrom AP, Gaur N, De Almeida AC, Skapura DG, Rudy Y, Burns AR, et al. (2011): Disrupted junctional membrane complexes and hyperactive ryanodine receptors after acute junctophilin knockdown in mice. Circulation **123,** 979-988
https://doi.org/10.1161/CIRCULATIONAHA.110.006437
Woo JS, Kim DH, Allen PD, Lee EH (2008): TRPC3-interacting triadic proteins in skeletal muscle. Biochem. J. **411,** 399-405
https://doi.org/10.1042/BJ20071504
Woo JS, Hwang JH, Ko JK, Kim DH, Ma J, Lee EH (2009): Glutamate at position 227 of junctophilin-2 is involved in binding to TRPC3. Mol. Cell. Biochem. **328,** 25-32
https://doi.org/10.1007/s11010-009-0070-0

Received: September 9, 2021
Final version accepted: December 8, 2021